iScience

CellPress
OPEN ACCESS

Article

JUN mediates glucocorticoid resistance by stabilizing HIF1a in T cell acute lymphoblastic leukemia

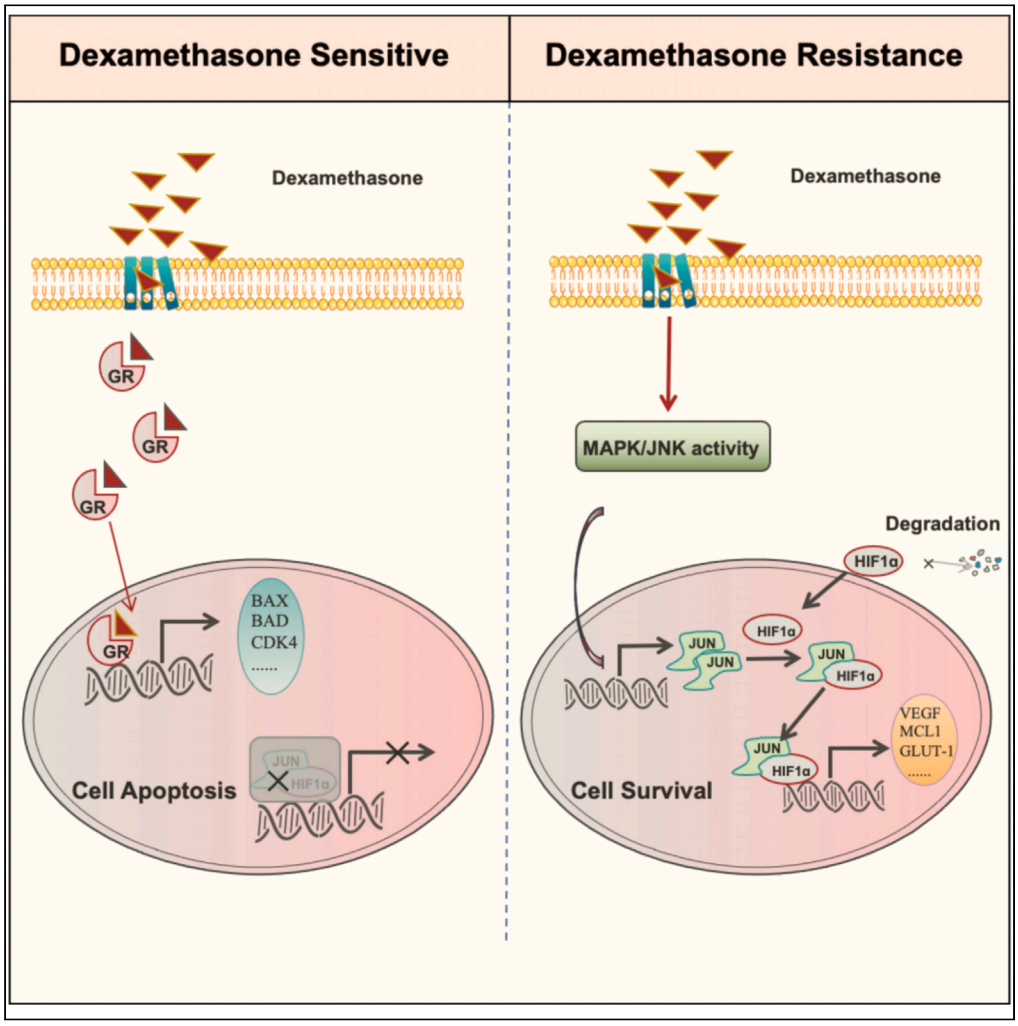

Zhijie Zhang, Jiangzhou Shi, Qifang Wu, ..., Tongcun Zhang, Fuling Zhou, Haichuan Zhu

zhangtongcun@wust.edu.cn (T.Z.)
zhoufuling@163.com (F.Z.)
zhuhaichuan@wust.edu.cn (H.Z.)

Highlights

JUN and HIF1α expression significantly upregulated in dexamethasone resistance T-ALL

JUN inhibits the degradation of HIF1α, mediating dexamethasone resistance in T-ALL

HIF1α could be a marker to predicate the dexamethasone resistance in clinical patients

Zhang et al., iScience 26, 108242
November 17, 2023
https://doi.org/10.1016/j.isci.2023.108242

iScience

CellPress
OPEN ACCESS

Article

JUN mediates glucocorticoid resistance by stabilizing HIF1a in T cell acute lymphoblastic leukemia

Zhijie Zhang,[1,5] Jiangzhou Shi,[1,5] Qifang Wu,[1] Zijian Zhang,[1] Xiaoyan Liu,[2] Anqi Ren,[1] Guanlin Zhao,[1] Ge Dong,[1] Han Wu,[1] Jiaxuan Zhao,[3] Yuan Zhao,[1] Jia Hu,[1] Hui Li,[4] Tongcun Zhang,[1,3,*] Fuling Zhou,[2,*] and Haichuan Zhu[1,6,*]

SUMMARY

Dexamethasone (Dex) plays a critical role in T-ALL treatment, but the mechanisms of Dex resistance are poorly understood. Here, we demonstrated that the expression of JUN was regulated in Dex-resistant T-ALL cell lines and patient samples. JUN knockdown increased the sensitivity to Dex. Moreover, the survival data showed that high expression of JUN related to poor prognosis of T-ALL patients. Then, we generated dexamethasone-resistant clones and conducted RNA-seq and ATAC-seq. We demonstrated that the upregulation of JUN was most significant and regulated by JNK pathway in Dex-resistant cells. High-throughput screening showed that HIF1α inhibitors synergized with Dex could enhance Dex resistance cells death *in vitro* and *in vivo*. Additionally, JUN combined and stabilized HIF1α in Dex resistance cells. These results reveal a new mechanism of Dex resistance in T-ALL and provide experimental evidence for the potential therapeutic benefit of targeting the JNK-JUN-HIF1α axis for T-ALL treatment.

INTRODUCTION

T cell acute lymphoblastic leukemia (T-ALL), a hematological malignancy derived from T cell progenitors, accounts for approximately 10%–15% of pediatric and 20%–25% of adult ALL cases.[1,2] Although intensive protocols have greatly improved, the relapsed or refractory rates remain above 40% in adults and 15% in children.[3,4] Administration of glucocorticoids (GCs), including prednisone, prednisolone, or dexamethasone, is an important part of T-ALL treatment, and resistance to dexamethasone is the main recurrent cause for a high relapse and death rate during treatment of T-ALL.[5] Thus, a better understanding of the mechanisms leading to dexamethasone resistance may identify biomarkers and targets that potentially improve T-ALL clinical therapy.

Dexamethasone is an anti-inflammatory drug widely used in acute lymphoblastic leukemia and other hematologic malignancies.[6–8] Prior studies have indicated that dexamethasone binds to the cytoplasmic GC receptor (GR) to form a heterodimer that translocated from the cytosol to the nucleus, where it transactivates or transrepresses target genes, leading to cell-cycle arrest and apoptosis.[7,9] Despite the clinical applications of this drug, the exact mechanisms involved in GC cytotoxicity and the development of resistance remain to be clarified. In T-ALL, the acquisition of abnormal expression of NR3C1, which encodes GR, is a frequent cause of GC resistance and is usually found in cell lines but rarely found in primary samples of GC-resistant patients.[10–12] In addition, several studies have shown that massive transcriptional activity induced by dexamethasone can contribute to drug resistance independent of GR expression, such as activation of glycolysis,[13] increased oxidative phosphorylation,[14] and activation of the PI3K/AKT/mTOR[15–18] and MYC signaling pathways.[19] To overcome the resistance of dexamethasone, many combinatorial approaches of specific inhibitors targeting these activity pathways have been developed and have shown promising results. However, it is uncertain how these findings might be translated into actionable therapeutic interventions.

JUN, which is an essential component of activating protein-1 (AP-1), was primarily reported as a proto-oncoprotein that regulates cell proliferation, apoptosis, and metastasis.[20] Previous studies have demonstrated that AP-1, which is composed of the JUN/FOS/JUNB family of homo and heterodimers, is involved in relevant cross-talk between GR and showed that JUN was upregulated by dexamethasone treatment and played an essential role in dexamethasone-induced apoptosis and that the overexpression of *c-Jun* could induce cell death in B cell leukemia.[21] However, others reported that the AP-1 transcription factor JUNB is essential for multiple myeloma cell proliferation and dexamethasone resistance,[22] indicating that the outcome of transcriptional regulation through AP-1/GR crosstalk depends on the state of signaling

[1]Institute of Biology and Medicine, College of Life and Health Sciences, Wuhan University of Science and Technology, Wuhan 430081, China
[2]Department of Hematology, Zhongnan Hospital of Wuhan University, Wuhan 430071, China
[3]Key Lab of Industrial Fermentation Microbiology of the Ministry of Education & Tianjin Key Lab of Industrial Microbiology, College of Biotechnology, Tianjin University of Science and Technology, Tianjin 300457, China
[4]Tianyou Hospital affiliated to Wuhan University of Science and Technology, Wuhan 430064, China
[5]These authors contributed equally
[6]Lead contact
*Correspondence: zhangtongcun@wust.edu.cn (T.Z.), zhoufuling@163.com (F.Z.), zhuhaichuan@wust.edu.cn (H.Z.)
https://doi.org/10.1016/j.isci.2023.108242

pathways and the subtype of disease. Although the mechanisms regulating the transcriptional activity of JUN by dexamethasone have been investigated in depth, the role of JUN expression in the regulation of drug resistance has not been examined in T-ALL.

In our study, we found that JUN was upregulated and essential for the survival of dexamethasone-resistant T-ALL cells. In terms of the mechanism, we identified that JUN stabilizes hypoxia-inducible factor-1α (HIF1α) due to direct protein-protein interactions and mediates dexamethasone resistance in T-ALL. We also revealed the major causes by which the c-Jun NH2-terminal protein kinase (JNK) pathway regulates *c-Jun* upregulation at the transcriptional level and further found that targeting HIF1α could synergistically overcome drug resistance. In short, we explored the possible mechanism of JNK-JUN-HIF1α-mediated T-ALL dexamethasone resistance and further provided possible strategies for drug resistance therapy in clinical T-ALL patients.

RESULTS

JUN is upregulated in dexamethasone-resistant T-ALL cells and correlates with poor prognosis in patients

Glucocorticoid resistance is particularly frequent in T-ALL and has been associated with poor survival.[23] In an effort to identify potential targets for glucocorticoid resistance in T-ALL, we compared the gene expression profiles of 16 GC-resistant T-ALL patient samples with those of 13 GC-sensitive T-ALL patient samples determined in a previous study.[24] A total of 727 genes were significantly enriched with more than 0.5-fold upregulation in GC-resistant T-ALL after correction for multiple hypothesis testing ($p < 0.05$) (Figure 1A, left). The datasets showed that AP-1 transcription factor (TF) family members, such as *Fos*, *FosB*, *Fosl1*, *Fosl2*, *and c-Jun*, were highly expressed in GC-resistant T-ALL (Figure 1A, right). Additionally, within the cohort of T-ALL cases, only *c-Jun* was significantly more highly expressed in T-ALL than in normal bone marrow, and *c-Jun* expression was significantly associated with survival outcomes in T-ALL patients (Figures 1B and S1).

Next, we compared the sensitivity to dexamethasone (Dex) in the T-ALL cell lines, and the IC50 values for the inhibition of T-ALL cell survival were as follows: MOLT-16 (61.9 μM), MOLT-3 (61.3 μM), MOLT-4 (60.4 μM), Jurkat (47.3 μM), Peer (16.2 μM), CUTLL-1 (3.5 μM), Loucy (2.4 μM), and CCRF-CEM (0.4 μM). It is consistent with previous studies showing that CCRF-CEM is dexamethasone sensitive (Figure 1C). To confirm the role of *c-Jun* in the process of T-ALL Dex resistance, we examined the IC50 of Dex and mRNA levels in different T-ALL cell lines and found that there were correlations with the efficacy of Dex but not significant (Figure 1D). After silencing JUN in Jurkat cells through RNA interference, Dex-resistant T-ALL cells were observably impaired (Figure 1E), and overexpressing JUN could significantly reduce the inhibitory effect of Dex on CCRF-CEM cell viability (Figure 1F). Taken together, these results suggest that JUN overexpression plays a critical role in dexamethasone resistance in T-ALL.

JNK/JUN axis activation contributed to drug resistance in T-ALL

To investigate the molecular mechanism underlying JUN upregulation in Dex-resistant cell lines, we first established a Dex-resistant T-ALL cell line by stepwise increases in the concentration of dexamethasone added to the drug-sensitive T-ALL cell line CCRF-CEM over a period of two months as described in the Methods (Figure 2A). The MTT assay showed that the IC50 values of dexamethasone for CCRF-CEM cells and CCRF-CEM(Dex) cells were 0.4 and 1000 μM, respectively, and the growth curves of the daughter cell line were similar to those of the parent cell line (Figures 2B and S2A). As expected, JUN was upregulated at both the translation and transcription levels in CCRF-CEM(Dex) cells, and the IC50 values of dexamethasone were significantly correlated with the JUN protein level (Figures 2C and 2D). We also found that antiapoptotic genes such as BAX and BCL-XL were upregulated in drug-resistant cells but decreased after dexamethasone treatment in sensitive T-ALL cells, which indicated that a dexamethasone-resistant cell line was successfully established (Figure S2B).

Then, we performed RNA-seq and ATAC-seq to investigate the molecular mechanism underlying *c-Jun* upregulation in CCRF-CEM cells and CCRF-CEM(Dex) cells. The differentially expressed genes were consistent with the patient results that *c-Jun*, Fosb, and *Fos* were upregulated in the dexamethasone-resistant cell line (Figure 2E), but apoptosis-related genes were downregulated in CCRF-CEM(Dex) cells after dexamethasone treatment (Figure S2C). Moreover, the enrichment of upregulated transcription factor analysis showed that *c-Jun* was significantly more active in Dex-resistant cells than in Dex-sensitive cell lines (Figure 2F). In addition, the average ATAC-seq signal around the transcription start sites was not significantly changed in CCRF-CEM(Dex) cells (Figures S2D–S2E). However, after screening the motifs of transcription factors that were significantly enriched using ATAC-seq data synchronously, we discovered that AP-1 and its relative transcription factors, such as JUN, FOS, and JUNB, were obviously enriched in CCRF-CEM(Dex) cells (Figure 2G). Together with the significant upregulation of genes in both CCRF-CEM(Dex) groups, we found that only three common TFs were shared in all three groups, and the top was JUN (Figure 2H). Subsequently, we examined the change in the JUN and downstream gene promoter region and found that JUN, JUNB, and FOSL1 (reliable JUN downstream gene) chromatin accessibility was enhanced in resistant cells (Figure S2F).

Several studies have demonstrated that the mitogen-activated protein kinase (MAPK) signaling pathways, including extracellular-regulated protein kinases 1 and 2 (ERK1/2), JNK, and p38 MAPK, regulate *c-Jun* gene expression,[25] which is consistent with our results that the MAPK pathway had a significant upward trend in the dexamethasone-resistant cell group (Figure 2I). Real-time PCR quantification and immunoblot analysis showed that JNK but not p38 MAPK activity or ERK1/2 activation was essential for the basal expression of *c-Jun* in resistant cells (Figures 2J and 2K). Compared to the p38 MAPK inhibitor SB203580 and ERK1/2 inhibitor SCH772984, only the JNK inhibitor SP600125 and AP-1 inhibitor aristolochic acid enhanced the antitumor activity in CCRF-CEM(Dex) cells (Figure 2L). Altogether, these results indicate that JNK activity is required for the regulation of *c-Jun* expression in dexamethasone-resistant T-ALL cells.

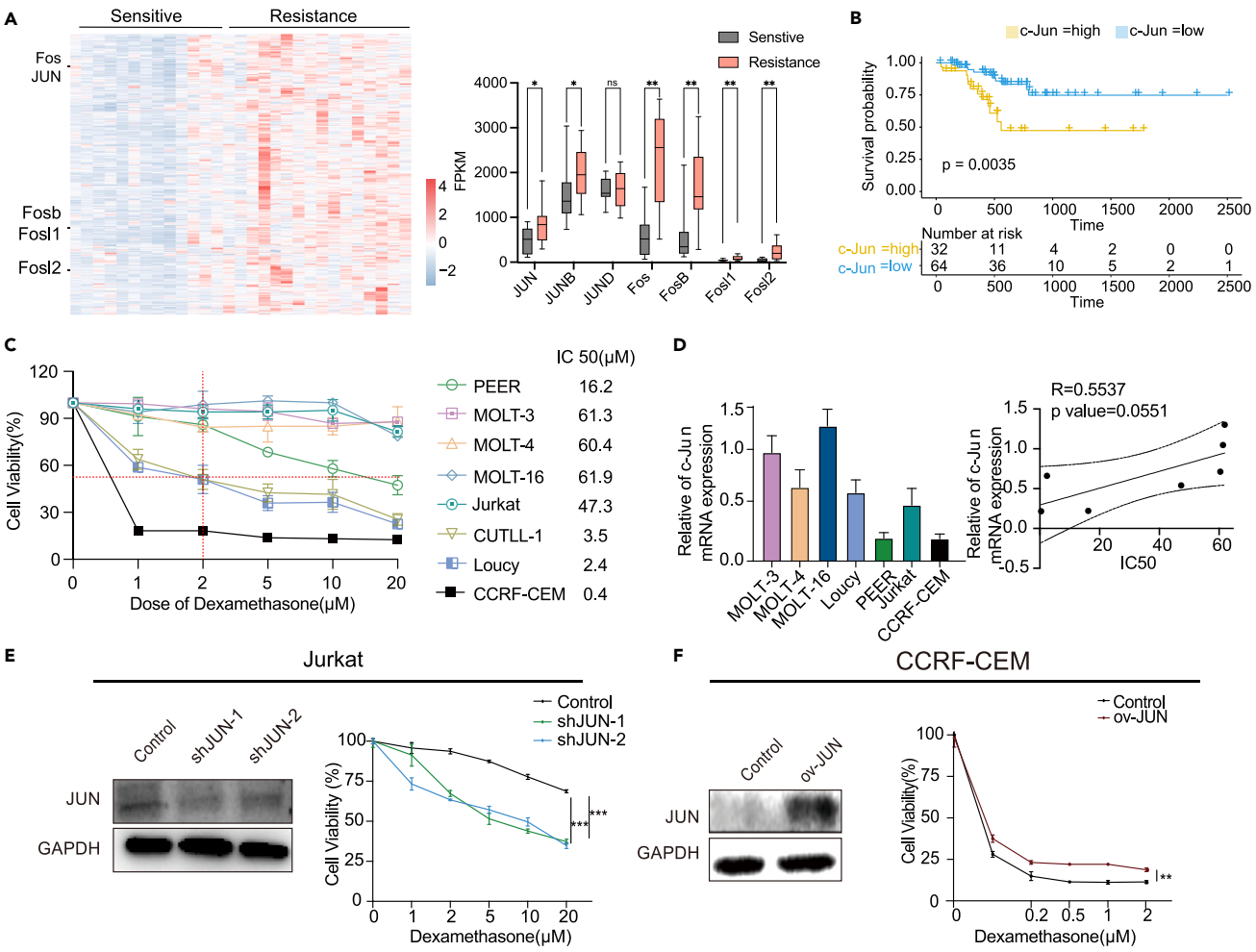

Figure 1. JUN plays a critical role in dexamethasone resistance in T-ALL cells

(A) Heatmap depicting 727 upregulated genes in a T-ALL cohort (GEO, GSE5820) (left). Upregulated genes were selected with $p < 0.05$ and log2 fold change >0.5 (left). Fragments per kilobase million (FPKM) of AP-1 TF family members (*Jun*, *Fos*, *Fosl1*, *Fosl2*, *FosB*) in a T-ALL cohort with 16 GC-resistant T-ALL patient samples and 13 GC-sensitive T-ALL patient samples (GEO, GSE5820) (right).

(B) Event-free survival of T-ALL patients with higher or lower expression of *c-Jun*, data from TARGET, phs000464.

(C) The relative cell viability of T-ALL cell lines. Cell counting was performed at 48 h after treatment with different concentration gradients of dexamethasone, and the IC50 was calculated as the concentration of dexamethasone that caused 50% cell death.

(D) Relative mRNA expression of *c-Jun* in T-ALL cell lines through qPCR (left) and the correlation between the IC50 values and the relative mRNA expression of *c-Jun* in T-ALL cell lines (right).

(E) The knockdown efficiency of JUN in Jurkat cells. Cells were harvested 72 h after transfection using lentivirus vectors, and a nontarget lentivirus vector (control) was used as the negative control (left). Cells were treated with different concentrations of dexamethasone, and cell counting was performed 48 h after treatment.

(F) Overexpression efficiency of JUN in CCRF-CEM cells. Cells were harvested 72 h after transfection using lentivirus vectors. A nontarget lentivirus vector (control) was used as the negative control (left). Cells were treated with different concentrations of dexamethasone, and cell counting was performed 48 h after treatment (right). Data are represented as mean ± SD (*$p < 0.05$, **$p < 0.01$, ***$p < 0.005$, ns = no significant).

JUN mediates the increased protein stability of HIF1α

Next, to explore the strategy of concomitant medications to overcome dexamethasone resistance therapeutically, we performed drug screening (2059 FDA-approved drugs). After two rounds of screening, 12 drugs were more sensitive to Dex-resistant cell lines (Figure S3A). The targets of these drugs were significantly enriched in angiogenesis and HIF1α signaling (Figure S3B), and the Dex-resistant cell lines Jurkat, MOLT-4, and CCRF-CEM(Dex) were more sensitive to the HIF1α inhibitors KC7F2 and BAY-872243 than CCRF-CEM (Figure 3A). The combination of Dex and several HIF1α inhibitors, such as KC7F2 and 2-methoxyestradiol, significantly inhibited the viability of CCRF-CEM(Dex), which was identified with a coefficient of drug interaction < 1 (Figure S3C).

Through the enrichment of gene expression and signaling pathway analysis, HIF1α was not significantly changed in Dex-resistant cells, but HIF1α downstream target genes had high expression compared to CCRF-CEM cells (Figure S3D). Pathway enrichment results showed that

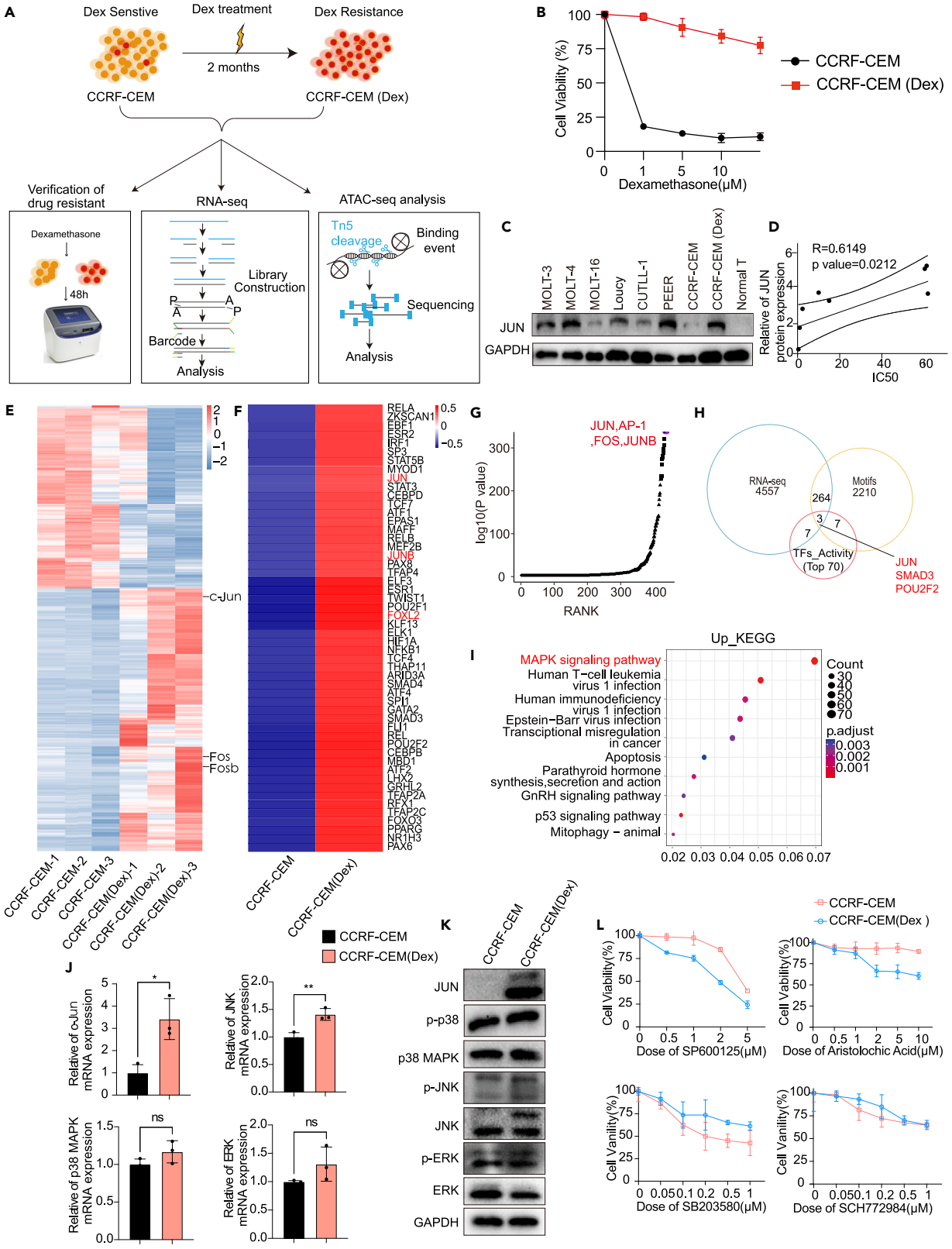
A
Dex Senstive
Dex treatment
Dex Resistance
2 months
CCRF-CEM
CCRF-CEM (Dex)
Verification of drug resistant
Dexamethasone
48h
RNA-seq
Library Construction
Barcode
Analysis
ATAC-seq analysis
Tn5 cleavage
Binding event
Sequencing
Analysis
B
Cell Viability (%)
Dexamethasone(μM)
CCRF-CEM
CCRF-CEM (Dex)
C
MOLT-3
MOLT-4
MOLT-16
Loucy
CUTLL-1
PEER
CCRF-CEM
CCRF-CEM (Dex)
Normal T
JUN
GAPDH
D
R=0.6149
p value=0.0212
Relative of JUN protein expression
IC50
E
c-Jun
Fos
Fosb
CCRF-CEM-1
CCRF-CEM-2
CCRF-CEM-3
CCRF-CEM(Dex)-1
CCRF-CEM(Dex)-2
CCRF-CEM(Dex)-3
F
CCRF-CEM
CCRF-CEM(Dex)
G
JUN,AP-1 ,FOS,JUNB
log10(P value)
RANK
H
RNA-seq 4557
Motifs 2210
264
TFs_Activity (Top 70)
JUN
SMAD3
POU2F2
I
Up_KEGG
MAPK signaling pathway
Human T-cell leukemia virus 1 infection
Human immunodeficiency virus 1 infection
Epstein-Barr virus infection
Transcriptional misregulation in cancer
Apoptosis
Parathyroid hormone synthesis,secretion and action
GnRH signaling pathway
p53 signaling pathway
Mitophagy - animal
Count
p.adjust
J
CCRF-CEM
CCRF-CEM(Dex)
Relative of cJun mRNA expression
Relative of JNK mRNA expression
Relative of p38 MAPK mRNA expression
Relative of ERK mRNA expression
ns
K
CCRF-CEM
CCRF-CEM(Dex)
JUN
p-p38
p38 MAPK
p-JNK
JNK
p-ERK
ERK
GAPDH
L
CCRF-CEM
CCRF-CEM(Dex)
Cell Viability(%)
Dose of SP600125(μM)
Dose of Aristolochic Acid(μM)
Dose of SB203580(μM)
Dose of SCH772984(μM)

Figure 2. JNK regulated JUN in dexamethasone-resistant T-ALL cells

(A) Schematic outline of drug-resistant stable cell line (CCRF-CEM(Dex)) generation, RNA-seq and ATAC-seq.

(B) The relative cell viability of CCRF-CEM and CCRF-CEM(Dex) cells. Cell counting was performed 48 h after treatment with different concentration gradients of dexamethasone.

(C) Protein levels of JUN in T-ALL cell lines determined by western blotting. GAPDH was used as an internal control.

(D) Correlation between the IC50 values and the protein expression of JUN in T-ALL cell lines.

(E) Heatmap depicting the differentially expressed genes (DEGs) between CCRF-CEM and CCRF-CEM(Dex) cells based on RNA-seq data. The color indicates the *Z* score of the expression of different genes. Genes were selected with $p < 0.05$ and log2 fold change >0.5.

(F) Top 70 significantly activated transcription factors (TFs) in each group based on RNA-seq data. The color indicates the *Z*-scaled average TF activity score.

(G) Rank of motifs enriched in the promoter region based on ATAC-seq.

(H) Venn diagram depicting the number of common genes in different groups. "Motifs" was the group of motifs enriched in the promoter, "RNA-seq" was the upregulated genes based on RNA-seq data, and "TF activity (Top 70)" was the group of the top 70 differentially activated TFs based on RNA-seq data.

(I) KEGG pathway analysis of upregulated genes in the CCRF-CEM(Dex) groups.

(J) Relative mRNA expression of JNK, ERK, and p38 MAPK in CCRF-CEM and CCRF-CEM(Dex) cells.

(K) Protein levels of JNK, ERK, p38 MAPK, phosphorylation level of ERK, phosphorylation level of JNK, and phosphorylation level of p38 MAPK in CCRF-CEM and CCRF-CEM(Dex) cells. GAPDH was used as the internal control.

(L) The relative cell viability of CCRF-CEM or CCRF-CEM(Dex) cells. Cell counting was performed at 48 h after treatment with different concentration gradients of aristolochic acid, SP600125, SB203580, and SCH772984. Data are represented as mean ± SD (*$p < 0.05$, **$p < 0.01$, ns = no significant).

HIF1α and HIF2α target-related pathways were significantly increased in Dex-resistant cells (Figure 3B). Consistently, real-time PCR quantification and immunoblot analysis showed that only the protein level of HIF1α but not the transcription level was significantly upregulated in the Dex-resistant cells, and the IC50 values of dexamethasone only correlated with the HIF1α protein level (Figures 3C and 3D). Additionally, to explore the underlying mechanism associated with the role of HIF1α in the Dex resistance of T-ALL cells, Jurkat and CCRF-CEM(Dex) cells were transfected with siHIF1α#1, siHIF1α#2, or their corresponding negative controls, while CCRF-CEM cells were transfected with HIF1α overexpression vector plasmid. The results from Figure 3 show that HIF1α interference observably diminished the cell viability of both Jurkat and CCRF-CEM(Dex) cells treated with Dex at concentrations ranging from 1 to 20 μM (Figures 3E and S3E), and overexpression of HIF1α notably rescued cell death (Figure S3F). Then, to evaluate the potential therapeutic effect of a HIF1α inhibitor in T-ALL, we performed experiments using CDX models created by CCRF-CEM(Dex) cells. As the schematic diagram shows, a total of 20 NCG mice were randomly assigned to four groups: control, dexamethasone (15 mg/kg/2 days), HIF1α inhibitor 2-methoxyestradiol (30 mg/kg/2 days), and dexamethasone combined with HIF1α inhibitor groups. All the groups were treated from day 6 to day 20 (Figure 3F). The survival time of xenografts was extended in the combination group but not in the Dex or 2-methoxyestradiol treatment groups (Figure 3G). We also analyzed bone marrow invasion through flow cytometry analysis and found that both Dex and HIF1α inhibitors could not significantly prevent leukemia cells from invading the bone marrow compared to the combined group (Figure 3H). Similarly, quantitative results showed that the combination group had stronger prevention of leukemia cells in peripheral blood and bone marrow (Figure 3I). Together, HIF1α is an important transcription factor that mediates Dex resistance in T-ALL cell lines, and inhibiting HIF1α enhances the effect of Dex on T-ALL cell lines.

Since JUN and HIF1α expressions were upregulated in Dex-resistant T-ALL cells, we next performed experiments to examine the genetic regulatory relationship between these two key TF genes. The results revealed that knockdown of JUN significantly reduced the relative protein levels of HIF1α (Figure 3J), whereas silencing HIF1α did not influence JUN at either the transcriptional or translational level (Figures 3E and 3K), suggesting that JUN is a crucial upstream regulator of HIF1α at the translational level.

Then, we hypothesized that JUN regulates HIF1α based on the protein interaction, and endogenous and exogenous experiments demonstrated our hypothesis that HIF1α interacted with JUN in the Dex-resistant cell line (Figures 3L–3M). Moreover, we also found that HIF1α retarded protein degradation in CCRF-CEM(Dex) cells by a protein half-life experiment compared to the sensitive cell line (Figure 3N). According to the results described previously, we revealed that JUN binding with HIF1α mediates the stable expression of HIF1α which contributes to Dex resistance.

Pharmacological inhibition of HIF1α reverses glucocorticoid resistance in patient samples

Next, we hypothesized that combined inhibition of GR and HIF1α might be an effective treatment for primary T-ALLs. We confirmed that HIF1α was also upregulated in Dex-resistant patient samples and ETP-ALL, in which patients have a high risk of remission failure or hematological relapse (Figure 4A). Importantly, T-ALL patients with higher HIF1α expression were more prone to relapse or other adverse events and had shorter survival times than patients with lower expression (TARGET, phs000464) (Figure 4B).

To explore whether the previously described conclusions are consistent in the clinic, we examined 12 samples (T1-T12) from T-ALL patients collected at diagnosis. First, we examined the sensitivity of these leukemia to Dex *in vitro* and defined T1-T4 as sensitive samples with IC50 < 2 μM and T5-T12 as resistant samples with IC50 ≥ 2 μM (Figure 4C). We also confirmed that the protein levels of HIF1α and JUN were upregulated in resistant samples and that HIF1α had a significant correlation with the IC50 value of Dex but JUN did not (Figures 4D–4F). Next, we examined the sensitivity of these leukemias to Dex, the HIF1α inhibitor BAY872243, or combined treatment *in vitro*. We found that the combination treatment was significantly more effective in the resistant groups at inhibiting cell survival than single-agent treatment, whereas sensitive samples did not respond to BAY872243 (Figure 4G).

To examine the effects *in vivo*, we engrafted NCG mice with T5 primary T-ALL and initiated treatment after 10 days based on fluorescence labeling. As the schematic diagram shows, randomized groups were treated with vehicle, Dex or BAY872243, and Dex-BAY872243 from day

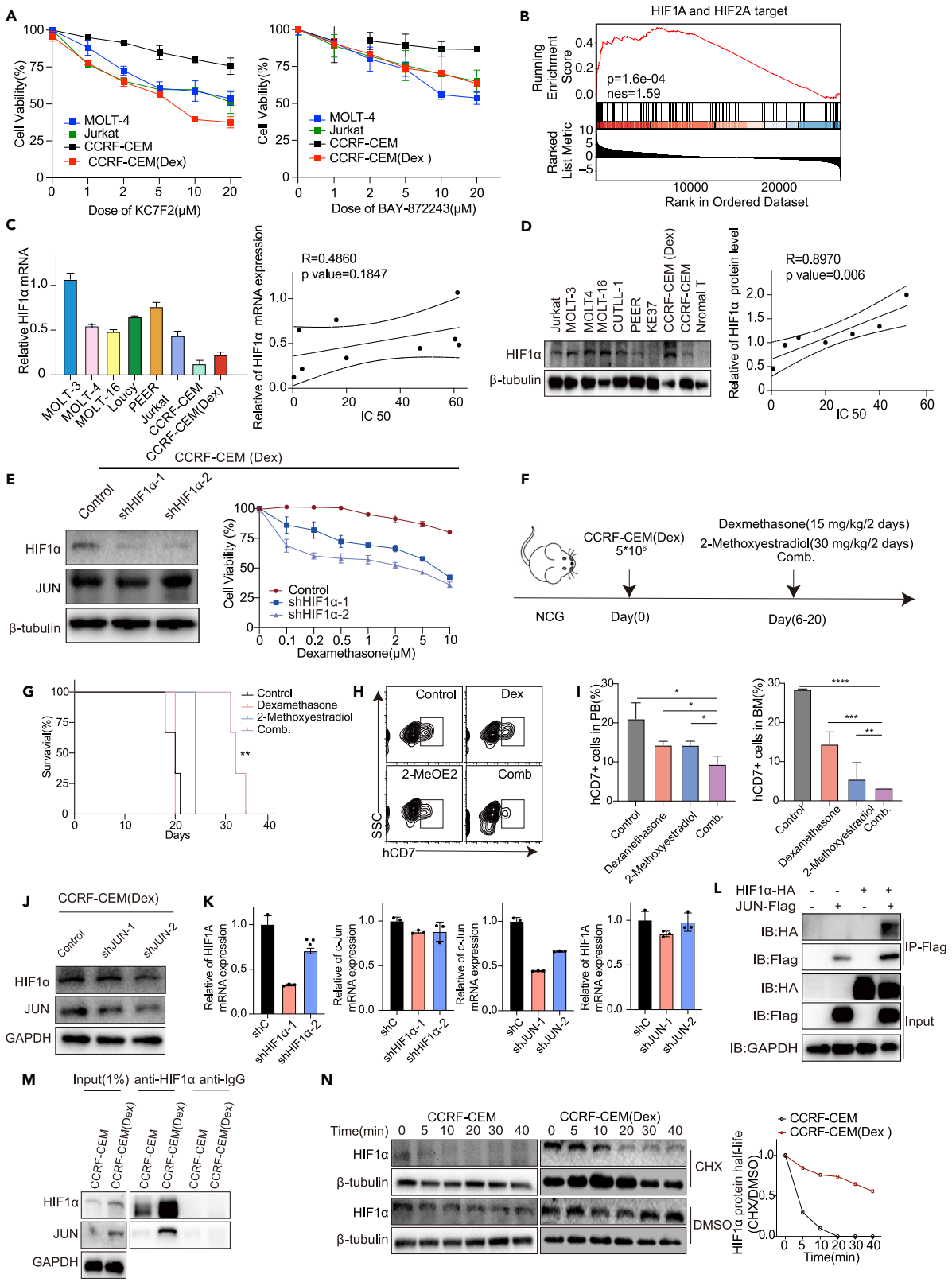
A
Cell Vability(%)
MOLT-4
Jurkat
CCRF-CEM
CCRF-CEM(Dex)
Dose of KC7F2(μM)
Dose of BAY-872243(μM)
B
HIF1A and HIF2A target
Running Enrichment Score
p=1.6e-04
nes=1.59
Ranked List Metric
Rank in Ordered Dataset
C
Relative HIF1α mRNA
MOLT-3
MOLT-4
MOLT-16
Loucy
PEER
Jurkat
CCRF-CEM
CCRF-CEM(Dex)
R=0.4860
p value=0.1847
Relative of HIF1α mRNA expression
IC 50
D
Jurkat
MOLT-3
MOLT4
MOLT-16
CUTLL-1
PEER
KE37
CCRF-CEM (Dex)
CCRF-CEM
Nromal T
HIF1α
β-tubulin
R=0.8970
p value=0.006
Relative of HIF1α protein level
IC 50
CCRF-CEM (Dex)
E
Control
shHIF1α-1
shHIF1α-2
HIF1α
JUN
β-tubulin
Cell Viability (%)
Control
shHIF1α-1
shHIF1α-2
Dexamethasone(μM)
F
CCRF-CEM(Dex)
5*10⁶
Dexmethasone(15 mg/kg/2 days)
2-Methoxyestradiol(30 mg/kg/2 days)
Comb.
NCG
Day(0)
Day(6-20)
G
Survaival(%)
Control
Dexamethasone
2-Methoxyestradiol
Comb.
Days
H
Control
Dex
2-MeOE2
Comb
SSC
hCD7
I
hCD7+ cells in PB(%)
hCD7+ cells in BM(%)
Control
Dexamethasone
2-Methoxyestradiol
Comb.
J
CCRF-CEM(Dex)
Control
shJUN-1
shJUN-2
HIF1α
JUN
GAPDH
K
Relative of HIF1A mRNA expression
Relative of c-Jun mRNA expression
shC
shHIF1α-1
shHIF1α-2
shJUN-1
shJUN-2
L
HIF1α-HA
JUN-Flag
IB:HA
IB:Flag
IP-Flag
Input
IB:GAPDH
M
Input(1%)
anti-HIF1α
anti-IgG
CCRF-CEM
CCRF-CEM(Dex)
HIF1α
JUN
GAPDH
N
CCRF-CEM
CCRF-CEM(Dex)
Time(min)
HIF1α
β-tubulin
CHX
DMSO
CCRF-CEM
CCRF-CEM(Dex)
HIF1α protein half-life (CHX/DMSO)
Time(min)

Figure 3. HIF1α is essential for dexamethasone resistance in T-ALL cells

(A) The relative cell viability of T-ALL cell lines. Cell counting was performed at 48 h after treatment with different concentration gradients of the HIF1a inhibitors KC7F2 (left) and BAY-872243 (right).

(B) Gene set enrichment analysis (GSEA) of upregulated genes in the CCRF-CEM(Dex) group.

(C) Relative mRNA expression of HIF1a in T-ALL cell lines through qPCR (left). The correlation between the IC50 values and the relative mRNA expression of HIF1a in T-ALL cell lines (right).

(D) Protein levels of HIF1a in T-ALL cell lines by western blot. GAPDH was used as an internal control (left), and the correlation between the IC50 values and the protein expression of HIF1a in T-ALL cell lines (right).

(E) The protein levels of HIF1a and JUN, CCRF-CEM(Dex) cells were harvested at 72 h after transfection with shHIF1a-1, shHIF1a-2, or nontarget lentivirus vectors (shC), β-tubulin was used as the internal control, CCRF-CEM(Dex) cells were treated with different concentrations of dexamethasone, and cell counting was performed at 48 h after treatment (right).

(F–I) CCRF-CEM(Dex) cell-derived xenograft (CDX) experiment in NCG mice, 5×10^6 CCRF-CEM(Dex) cells were injected through the tail vein, dexamethasone (15 mg/kg/2 days), 2-methoxyestradiol (30 mg/kg/2 days) or a combination of these two inhibitors was intraperitoneally administered from day 6 to 20, and the control group was treated with PBS.

(F) Schematic outline of cell-derived xenograft (CDX) generation.

(G) Kaplan–Meier survival curves of CCRF-CEM(Dex) cell-derived xenograft mice (CDX) in different treatment groups.

(H) Analysis of bone marrow invasion using anti-human CD7 antibody through flow cytometry.

(I) Quantification of peripheral blood and bone marrow invasion after drug treatment.

(J) The protein levels of HIF1a and JUN after JUN silencing in CCRF-CEM(Dex) and CCRF-CEM(Dex) cells were harvested 72 h after transfection with shJUN-1, shJUN-2, or nontarget lentivirus vectors (shC). GAPDH was used as the internal control.

(K) Relative mRNA expression of c-Jun or HIF1a in T-ALL cell lines through qPCR. CCRF-CEM(Dex) cells were harvested 72 h after transfection with shJUN-1, shJUN-2, shHIF1a-1, shHIF1a-2, or nontarget lentivirus vectors (shC).

(L and M) Verification of the interaction between JUN and HIF1a. (L) Co-IP of JUN and HIF1a from the lysates of transfected cells. HEK293T cells were cotransfected with the plasmid combination pcDNA3.1-JUN-Flag/pcDNA3.1-HIF1a-HA and measured by western blotting.

(M) Co-IP of JUN and HIF1a from the lysates of CCRF-CEM(Dex) cells. Cells were lysed, and co-IP assays were carried out and analyzed by western blotting.

(N) Cycloheximide (CHX) chase assays showing that HIF1a retarded protein degradation in CCRF-CEM(Dex) cells (left), quantification rate of degradation (right).

Data are represented as mean ± SD (*$p < 0.05$, **$p < 0.01$, ***$p < 0.005$, ****$p < 0.001$).

10 to day 30, and the real-time tumor burden and the effects on overall survival were determined (Figure 4H). Both BAY872243 and the combination group suppressed the growth of human T-ALL cells *in vivo* (Figure 4I). Similarly, the survival time of xenografts was significantly prolonged compared to treatment with vehicle or single-agent therapy for T-ALL (Figure 4J). We also analyzed bone marrow invasion through flow cytometry analysis and found that neither BAY872243 nor Dex significantly prevented leukemia cell invasion into the bone marrow compared to the combination group (Figure 4K). Together, HIF1α could be used as a prediction marker, and this combination of targeted therapies could augment current and emerging therapies for Dex-resistant T-ALL.

DISCUSSION

T-ALL is the most common malignancy in children and adults, and synthetic GCs such as dexamethasone and prednisolone are integral components in the treatment protocols of T-ALL.[5] Cellular resistance to dexamethasone is one of the most central causes of T-ALL relapse.[26,27] Although several potential targets have been explored, including PI3K/AKT,[28] mTOR,[29,30] NOTCH,[31] and CDK4/6,[32] to overcome GC resistance in T-ALL,[19] the biological mechanism behind GC resistance has not yet been fully elucidated. In the present study, JUN and HIF1α expression was found to be correlated with Dex resistance in T-ALL patients and cell lines. High expression of JUN and HIF1α predicts a poorer prognosis in T-ALL patients. JUN binds to HIF1α and induces its expression by inhibiting its degradation, thereby conferring cellular resistance to dexamethasone. Furthermore, interference with JUN or HIF1α expression by short hairpin RNA significantly reduced cell viability, while overexpression of either protein resulted in the opposite effect of Dex-induced cell death in CCRF-CEM cells.

JUN, as an immediate-early response gene, is regulated by extracellular stimulation, such as serum, phorbol esters, and glucocorticoids.[33] The increased expression of both *c-Jun* mRNA and protein is accompanied by the induction of GR expression.[34] It has been shown that c-Jun induction by Dex could be inhibited by the addition of a p38-MAPK inhibitor but not a JNK inhibitor.[21] In our study, *c-Jun* induction was primarily a transcriptional phenomenon in CCRF-CEM(Dex) cells, and we found that only JNK was activated in resistant cells. Treatment with SP600125, a JNK inhibitor, decreased JUN expression and increased cell death, indicating that the JNK pathway contributes to JUN-derived Dex drug resistance in T-ALL. Of note, the role of JUN between short-term treatment with Dex and Dex-resistant cell lines is different and requires further analysis.

The role of HIF1α in leukemia has been extensively studied at both the mRNA and protein levels, and increased expression of HIF1α has been found in various hematologic malignancies compared to normal cells.[35] Hypoxia and activation of HIF signaling play an important role in resistance mechanisms to chemotherapeutic agents, and the combination of chemotherapy targeting the hypoxic pathway may represent a valuable therapeutic approach for some types of leukemia.[36,37] However, the determinants of HIF1α regulation in the normoxic environment and the mechanism of Dex resistance are incompletely understood. Here, we found that HIF1α inhibitors were sensitive to Dex-resistant T-ALL cell lines and that there was a correlation between HIF1α protein expression and Dex sensitivity in cell lines. In addition, we found that JUN increased significantly in drug-resistant cell lines, revealing the interaction between JUN and HIF1α, which inhibited the expression of HIF1α normoxia degradation stable protein and mediated Dex resistance in cells. Our study is consistent with previous results showing that HIF1α

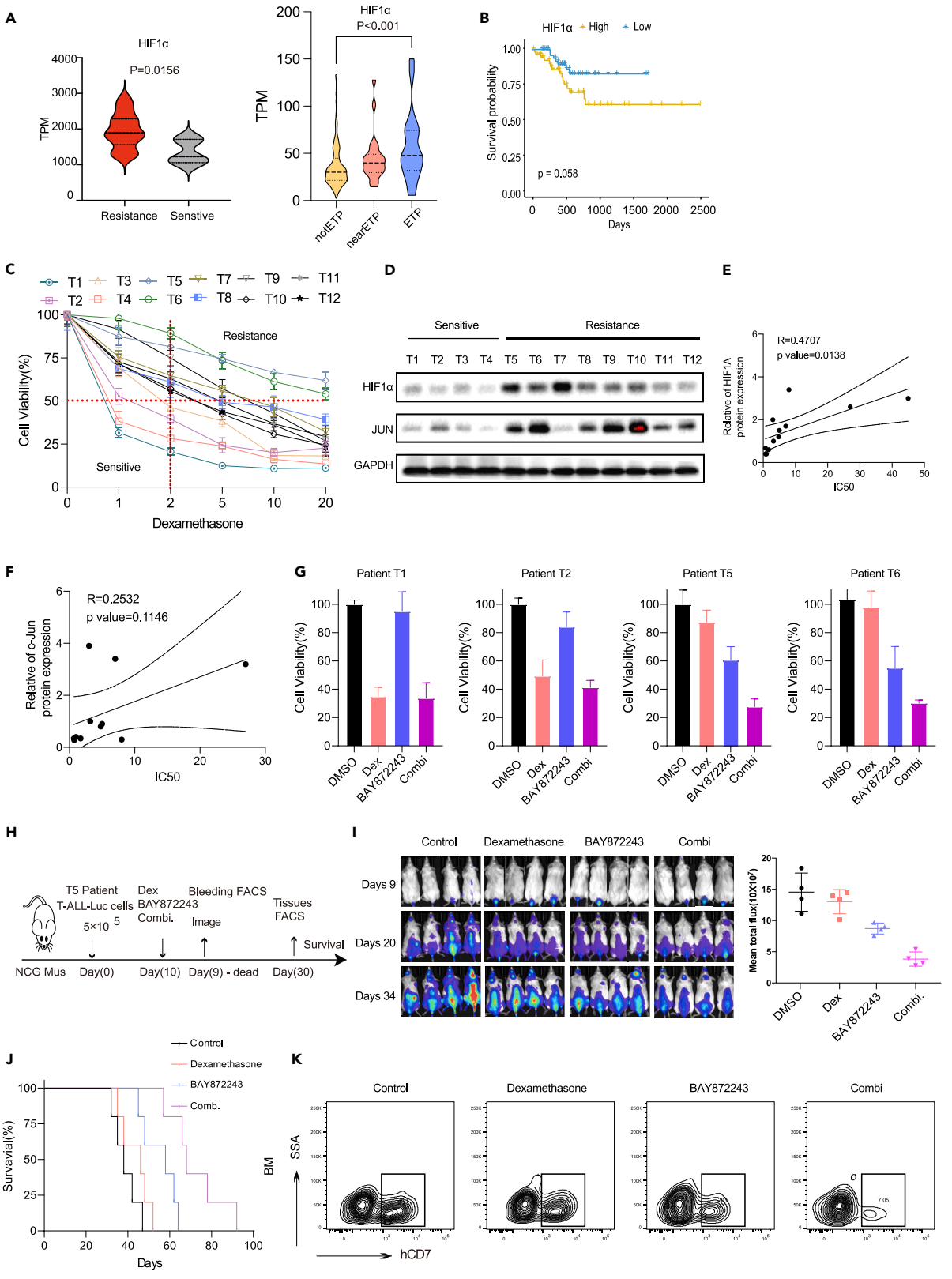
A
HIF1α
P=0.0156
TPM
Resistance
Senstive
HIF1α
P<0.001
TPM
notETP
nearETP
ETP
B
HIF1α High Low
Survival probability
p = 0.058
Days
C
T1 T2 T3 T4 T5 T6 T7 T8 T9 T10 T11 T12
Resistance
Sensitive
Cell Viability(%)
Dexamethasone
D
Sensitive
Resistance
T1 T2 T3 T4 T5 T6 T7 T8 T9 T10 T11 T12
HIF1α
JUN
GAPDH
E
R=0.4707
p value=0.0138
Relative of HIF1A protein expression
IC50
F
R=0.2532
p value=0.1146
Relative of c-Jun protein expression
IC50
G
Patient T1
Patient T2
Patient T5
Patient T6
Cell Viability(%)
DMSO
Dex
BAY872243
Combi
H
T5 Patient T-ALL-Luc cells
5×10 5
Dex
BAY872243
Combi.
Bleeding FACS
Image
Tissues FACS
Survival
NCG Mus
Day(0)
Day(10)
Day(9) - dead
Day(30)
I
Control
Dexamethasone
BAY872243
Combi
Days 9
Days 20
Days 34
Mean total flux(10X10⁷)
DMSO
Dex
BAY872243
Combi.
J
Control
Dexamethasone
BAY872243
Comb.
Survavial(%)
Days
K
Control
Dexamethasone
BAY872243
Combi
SSA
BM
hCD7

Figure 4. T-ALL patient samples with glucocorticoid resistance are sensitive to HIF1a inhibition

(A) TPM of HIF1a in the resistant and sensitive groups based on a T-ALL cohort (GEO, GSE5820) (left), TPM of HIF1a in different groups based on a T-ALL cohort including ETP-ALL and non-ETP-ALL patient samples (right).

(B) Event-free survival of T-ALL patients with higher or lower expression of HIF1a (TARGET, phs000464).

(C) The relative cell viability of blast cells from 12 T-ALL patients (T1-T12) treated with different concentration gradients of dexamethasone.

(D) Protein levels of HIF1a and JUN in T-ALL patient samples determined by western blotting. GAPDH was used as an internal control.

(E) The correlation between the IC50 values and the protein expression of JUN.

(F) The correlation between the IC50 values and the protein expression of HIF1α.

(G) Synergistic inhibition of Dex and BAY872243 in patient samples. Cell counting was performed at 48 h.

(H–K) T5 patient sample cell-derived xenograft (CDX) experiment in NCG mice, 5×10^5 luciferase-labeled T5 patient sample cells were injected through the tail vein, dexamethasone or BAY872243 or a combination of these two inhibitors from day 10 to day 30, and the control group was treated with PBS.

(H) Schematic outline of patient-derived xenografts (PDXs).

(I) Bioluminescent imaging of T5-derived xenograft mice in different treatment groups.

(J) Kaplan–Meier survival curves of xenograft mice (PDX) in different treatment groups.

(K) Analysis of bone marrow invasion using anti-human CD7 antibody through flow cytometry. Data are represented as mean ± SD.

levels impact T-ALL chemoresistance in hypoxia.[36,38] In addition, leukemia stem cells, which are regarded as the origins of leukemia and are resistant to standard chemotherapy, were shown to be dependent on a molecular loop implicating HIF1α and WNT/β-catenin, both of which are activated in hypoxia.[38] All of the previously described results indicate that HIF1α is an interesting therapeutic target, but its clinical application requires additional work.

Taken together, we describe HIF1α and JUN as essential for T-ALL Dex resistance. We also confirmed a correlation between HIF1α and JUN and identified the mechanism of HIF1α protein staining in a normoxic environment. Meanwhile, relapsed precursor patients with high HIF1α and JUN expression have a poor prognosis. Clinical sample experiments demonstrated that HIF1α inhibitors are insensitive to Dex-resistant samples. Our study describes a mechanism of Dex resistance, and preliminary clinical trials have demonstrated its feasibility in treating drug resistance in T-ALL, which needs to be confirmed by further clinical trials.

Limitations of the study

There are some possible limitations of our study. We mainly demonstrated the reasons for the upregulation of HIF1α expression from the protein levels, but the study of the mRNA level was lacking. In the future, the therapeutic effect of HIF1α inhibitor combined with dexamethasone after secondary drug resistance in clinical samples would be investigated to provide more experimental evidence for HIF1α as a clinical marker of dexamethasone resistance.

STAR★METHODS

Detailed methods are provided in the online version of this paper and include the following:

- KEY RESOURCES TABLE
- RESOURCE AVAILABILITY
  - Lead contact
  - Materials availability
  - Data and code availability
- EXPERIMENTAL MODEL AND STUDY PARTICIPANT DETAILS
  - Cell lines and growth condition
  - Patients samples
  - Mouse models
- METHOD DETAILS
  - Gene knockdown and overexpression
  - Real time PCR
  - Coimmunoprecipitation and western blot analysis
  - Flow cytometry
  - RNA-seq analysis
  - ATAC-seq analysis
  - Drug library screening
- QUANTIFICATION AND STATISTICAL ANALYSIS

SUPPLEMENTAL INFORMATION

Supplemental information can be found online at https://doi.org/10.1016/j.isci.2023.108242.

ACKNOWLEDGMENTS

We are obliged to Dr. Ningning Yao, Prof. Hong Wu (The MOE Key Laboratory of Cell Proliferation and Differentiation, Peking University), and Yuan Cao, and Piao Zou (Analytical & Testing Center, Wuhan University of Science and Technology) for their assistance in the experiments. This work was funded by grants from the Natural Science Foundation of Hubei Province (2022CFB029) and the National Natural Science Foundation of China (82100193) to H.Z., the Scientific Research Program for Young Talents of Hubei Provincial Department of Education (Q202111113) and Wuhan Knowledge Innovation Project, Dawn Plan (20220220208001020313) to H.L., Zhongnan Hospital of Wuhan University Science, Discipline and Platform Construction Fund (PDJH202217), Zhongnan Hospital of Wuhan University discipline construction platform project (grant number 202021), and Zhongnan Hospital of Wuhan University Science, Technology and Innovation Cultivation Fund (ZNLH201902) to F.Z.

AUTHOR CONTRIBUTIONS

H.Z., Z.Z., and F.Z. designed the experimental plans; Z.Z., J.S., Z.Z., X.L., A.R., G.D., H.W., Y.Z., H.L., and J.Z. performed the experiments. Q.W. performed the bioinformatic analysis; Z.Z. and H.Z. analyzed the data and drafted the manuscript. Z.Z., J.S., Z.Z., G.Z., and T.Z. were involved in the revision of the manuscript.

DECLARATION OF INTERESTS

No potential conflict of interests was reported by authors.

INCLUSION AND DIVERSITY

We support inclusive, diverse, and equitable conduct of research.

Received: September 5, 2023
Revised: September 23, 2023
Accepted: October 16, 2023
Published: October 18, 2023

REFERENCES

1. Belver, L., and Ferrando, A. (2016). The genetics and mechanisms of T cell acute lymphoblastic leukaemia. Nat. Rev. Cancer *16*, 494–507.
2. Hunger, S.P., and Mullighan, C.G. (2015). Acute lymphoblastic leukemia in children. N. Engl. J. Med. *373*, 1541–1552.
3. Pui, C.-H., Relling, M.V., and Downing, J.R. (2004). Acute lymphoblastic leukemia. N. Engl. J. Med. *350*, 1535–1548.
4. Trinquand, A., Tanguy-Schmidt, A., Ben Abdelali, R., Lambert, J., Beldjord, K., Lengliné, E., De Gunzburg, N., Payet-Bornet, D., Lhermitte, L., Mossafa, H., et al. (2013). Toward a NOTCH1/FBXW7/RAS/PTEN–based oncogenetic risk classification of adult t-cell acute lymphoblastic leukemia: A group for research in adult acute lymphoblastic leukemia study. J. Clin. Oncol. *31*, 4333–4342.
5. van der Zwet, J.C.G., Buijs-Gladdines, J.G.C.A.M., Cordo', V., Debets, D.O., Smits, W.K., Chen, Z., Dylus, J., Zaman, G.J.R., Altelaar, M., Oshima, K., et al. (2021). MAPK-ERK is a central pathway in T-cell acute lymphoblastic leukemia that drives steroid resistance. Leukemia *35*, 3394–3405.
6. Greenstein, S., Ghias, K., Krett, N.L., and Rosen, S.T. (2002). Mechanisms of glucocorticoid-mediated apoptosis in hematological malignancies. Clin. Cancer Res. *8*, 1681–1694.
7. Scheijen, B. (2019). Molecular mechanisms contributing to glucocorticoid resistance in lymphoid malignancies. Cancer Drug Resist. *2*, 647–664.
8. Bertoli, S., Picard, M., Bérard, E., Griessinger, E., Larrue, C., Mouchel, P.L., Vergez, F., Tavitian, S., Yon, E., Ruiz, J., et al. (2018). Dexamethasone in hyperleukocytic acute myeloid leukemia. Haematologica *103*, 988–998.
9. Toscan, C.E., Jing, D., Mayoh, C., and Lock, R.B. (2020). Reversal of glucocorticoid resistance in paediatric acute lymphoblastic leukaemia is dependent on restoring BIM expression. Br. J. Cancer *122*, 1769–1781.
10. Wandler, A.M., Huang, B.J., Craig, J.W., Hayes, K., Yan, H., Meyer, L.K., Scacchetti, A., Monsalve, G., Dail, M., Li, Q., et al. (2020). Loss of glucocorticoid receptor expression mediates in vivo dexamethasone resistance in T-cell acute lymphoblastic leukemia. Leukemia *34*, 2025–2037.
11. Zhu, H., Dong, B., Zhang, Y., Wang, M., Rao, J., Cui, B., Liu, Y., Jiang, Q., Wang, W., Yang, L., et al. (2022). Integrated genomic analyses identify high-risk factors and actionable targets in T-cell acute lymphoblastic leukemia. Blood Sci. *4*, 16–28.
12. Liu, Y., Easton, J., Shao, Y., Maciaszek, J., Wang, Z., Wilkinson, M.R., McCastlain, K., Edmonson, M., Pounds, S.B., Shi, L., et al. (2017). The genomic landscape of pediatric and young adult T-lineage acute lymphoblastic leukemia. Nat. Genet. *49*, 1211–1218.
13. Hulleman, E., Kazemier, K.M., Holleman, A., VanderWeele, D.J., Rudin, C.M., Broekhuis, M.J.C., Evans, W.E., Pieters, R., and Den Boer, M.L. (2009). Inhibition of glycolysis modulates prednisolone resistance in acute lymphoblastic leukemia cells. Blood. The Journal of the American Society of Hematology *113*, 2014–2021.
14. Samuels, A.L., Heng, J.Y., Beesley, A.H., and Kees, U.R. (2014). Bioenergetic modulation overcomes glucocorticoid resistance in T-lineage acute lymphoblastic leukaemia. Br. J. Haematol. *165*, 57–66.
15. Silveira, A.B., Laranjeira, A.B.A., Rodrigues, G.O.L., Leal, P.C., Cardoso, B.A., Barata, J.T., Yunes, R.A., Zanchin, N.I.T., Brandalise, S.R., and Yunes, J.A. (2015). PI3K inhibition synergizes with glucocorticoids but antagonizes with methotrexate in T-cell acute lymphoblastic leukemia. Oncotarget *6*, 13105–13118.
16. Piovan, E., Yu, J., Tosello, V., Herranz, D., Ambesi-Impiombato, A., Da Silva, A.C., Sanchez-Martin, M., Perez-Garcia, A., Rigo, I., Castillo, M., et al. (2013). Direct reversal of glucocorticoid resistance by AKT inhibition in acute lymphoblastic leukemia. Cancer Cell *24*, 766–776.
17. Bornhauser, B.C., Bonapace, L., Lindholm, D., Martinez, R., Cario, G., Schrappe, M., Niggli, F.K., Schäfer, B.W., and Bourquin, J.-P. (2007). Low-dose arsenic trioxide sensitizes glucocorticoid-resistant acute lymphoblastic leukemia cells to dexamethasone via an Akt-dependent pathway. Blood, The Journal of the American Society of Hematology *110*, 2084–2091.
18. Hall, C.P., Reynolds, C.P., and Kang, M.H. (2016). Modulation of Glucocorticoid Resistance in Pediatric T-cell Acute Lymphoblastic Leukemia by Increasing BIM Expression with the PI3K/mTOR Inhibitor BEZ235BEZ235 plus Dexamethasone in ALL. Clin. Cancer Res. *22*, 621–632.
19. Olivas-Aguirre, M., Torres-López, L., Pottosin, I., and Dobrovinskaya, O. (2021). Overcoming glucocorticoid resistance in acute lymphoblastic leukemia: repurposed drugs

can improve the protocol. Front. Oncol. *11*, 617937.

20. Wisdom, R., Johnson, R.S., and Moore, C. (1999). c-Jun regulates cell cycle progression and apoptosis by distinct mechanisms. The EMBO journal *18*, 188–197.
21. Heidari, N., Miller, A.V., Hicks, M.A., Marking, C.B., and Harada, H. (2012). Glucocorticoid-mediated BIM induction and apoptosis are regulated by Runx2 and c-Jun in leukemia cells. Cell Death Dis. *3*, e349.
22. Fan, F., Bashari, M.H., Morelli, E., Tonon, G., Malvestiti, S., Vallet, S., Jarahian, M., Seckinger, A., Hose, D., Bakiri, L., et al. (2017). The AP-1 transcription factor JunB is essential for multiple myeloma cell proliferation and drug resistance in the bone marrow microenvironment. Leukemia *31*, 1570–1581.
23. Beesley, A.H., Firth, M.J., Ford, J., Weller, R.E., Freitas, J.R., Perera, K.U., and Kees, U.R. (2009). Glucocorticoid resistance in T-lineage acute lymphoblastic leukaemia is associated with a proliferative metabolism. Br. J. Cancer *100*, 1926–1936.
24. Wei, G., Twomey, D., Lamb, J., Schlis, K., Agarwal, J., Stam, R.W., Opferman, J.T., Sallan, S.E., den Boer, M.L., Pieters, R., et al. (2006). Gene expression-based chemical genomics identifies rapamycin as a modulator of MCL1 and glucocorticoid resistance. Cancer Cell *10*, 331–342.
25. Johnson, G.L., and Lapadat, R. (2002). Mitogen-activated protein kinase pathways mediated by ERK, JNK, and p38 protein kinases. Science *298*, 1911–1912.
26. Kaspers, G.J.L., Wijnands, J.J.M., Hartmann, R., Huismans, L., Loonen, A.H., Stackelberg, A., Henze, G., Pieters, R., Hählen, K., Van Wering, E.R., and Veerman, A.J.P. (2005). Immunophenotypic cell lineage and in vitro cellular drug resistance in childhood relapsed acute lymphoblastic leukaemia. Eur. J. Cancer *41*, 1300–1303.
27. Kaspers, G.J., Pieters, R., Klumper, E., De Waal, F.C., and Veerman, A.J. (1994). Glucocorticoid resistance in childhood leukemia. Leuk. Lymphoma *13*, 187–201.
28. Piovan, E., Yu, J., Tosello, V., Herranz, D., Ambesi-Impiombato, A., Da Silva, A.C., Sanchez-Martin, M., Perez-Garcia, A., Rigo, I., Castillo, M., et al. (2013). Direct Reversal of Glucocorticoid Resistance by AKT Inhibition in Acute Lymphoblastic Leukemia. Cancer Cell *24*, 766–776.
29. Hall, C.P., Reynolds, C.P., and Kang, M.H. (2016). Modulation of Glucocorticoid Resistance in Pediatric T-cell Acute Lymphoblastic Leukemia by Increasing BIM Expression with the PI3K/mTOR Inhibitor BEZ235. Clin. Cancer Res. *22*, 621–632. https://doi.org/10.1158/1078-0432.Ccr-15-0114.
30. Gu, L., Zhou, C., Liu, H., Gao, J., Li, Q., Mu, D., and Ma, Z. (2010). Rapamycin sensitizes T-ALL cells to dexamethasone-induced apoptosis. J. Exp. Clin. Cancer Res. *29*, 150. https://doi.org/10.1186/1756-9966-29-150.
31. Real, P.J., Tosello, V., Palomero, T., Castillo, M., Sawai, C., Sulis, M.L., Meijerink, J.P., Basso, G., Aifantis, I., Cordon-Cardo, C., and Ferrando, A.A. (2008). Inhibition of NOTCH1 Signaling and Glucocorticoid Therapy in T-ALL. Blood *112*, 298.
32. Bortolozzi, R., Mattiuzzo, E., Trentin, L., Accordi, B., Basso, G., and Viola, G. (2018). Ribociclib, a Cdk4/Cdk6 kinase inhibitor, enhances glucocorticoid sensitivity in B-acute lymphoblastic leukemia (B-All). Biochem. Pharmacol. *153*, 230–241. https://doi.org/10.1016/j.bcp.2018.01.050.
33. Wei, P., Inamdar, N., and Vedeckis, W.V. (1998). Transrepression of c-jun gene expression by the glucocorticoid receptor requires both AP-1 sites in the c-jun promoter. Mol. Endocrinol. *12*, 1322–1333.
34. Barrett, T.J., Vig, E., and Vedeckis, W.V. (1996). Coordinate regulation of glucocorticoid receptor and c-jun gene expression is cell type-specific and exhibits differential hormonal sensitivity for down-and up-regulation. Biochemistry *35*, 9746–9753.
35. Wang, Y., Liu, Y., Malek, S.N., Zheng, P., and Liu, Y. (2011). Targeting HIF1α Eliminates Cancer Stem Cells in Hematological Malignancies. Cell Stem Cell *8*, 399–411.
36. Fahy, L., Calvo, J., Chabi, S., Renou, L., Le Maout, C., Poglio, S., Leblanc, T., Petit, A., Baruchel, A., Ballerini, P., et al. (2021). Hypoxia favors chemoresistance in T-ALL through an HIF1α-mediated mTORC1 inhibition loop. Blood Adv. *5*, 513–526.
37. Muz, B., De La Puente, P., Azab, F., Luderer, M., and Azab, A.K. (2014). The Role of Hypoxia and Exploitation of the Hypoxic Environment in Hematologic MalignanciesHypoxia in Hematologic Malignancies. Mol. Cancer Res. *12*, 1347–1354.
38. Giambra, V., Jenkins, C.E., Lam, S.H., Hoofd, C., Belmonte, M., Wang, X., Gusscott, S., Gracias, D., and Weng, A.P. (2015). Leukemia stem cells in T-ALL require active Hif1α and Wnt signaling. Blood, The Journal of the American Society of Hematology *125*, 3917–3927.
39. Ramírez, F., Ryan, D.P., Grüning, B., Bhardwaj, V., Kilpert, F., Richter, A.S., Heyne, S., Dündar, F., and Manke, T. (2016). deepTools2: a next generation web server for deep-sequencing data analysis. Nucleic Acids Res. *44*, W160–W165. https://doi.org/10.1093/nar/gkw257.
40. John, M.G. (2018). Improved peak-calling with MACS2. Preprint at bioRxiv. https://doi.org/10.1101/496521.
41. Robinson, J.T., Thorvaldsdóttir, H., Winckler, W., Guttman, M., Lander, E.S., Getz, G., and Mesirov, J.P. (2011). Integrative genomics viewer. Nat. Biotechnol. *29*, 24–26. https://doi.org/10.1038/nbt.1754.
42. Langmead, B., and Salzberg, S.L. (2012). Fast gapped-read alignment with Bowtie 2. Nat. Methods *9*, 357–359. https://doi.org/10.1038/nmeth.1923.
43. Li, H., Handsaker, B., Wysoker, A., Fennell, T., Ruan, J., Homer, N., Marth, G., Abecasis, G., and Durbin, R.; 1000 Genome Project Data Processing Subgroup (2009). The Sequence Alignment/Map format and SAMtools. Bioinformatics *25*, 2078–2079. https://doi.org/10.1093/bioinformatics/btp352.
44. Liao, Y., Smyth, G.K., and Shi, W. (2014). featureCounts: an efficient general purpose program for assigning sequence reads to genomic features. Bioinformatics *30*, 923–930. https://doi.org/10.1093/bioinformatics/btt656.
45. Love, M. I., Huber, W., and Anders, S. (2014). Moderated estimation of fold change and dispersion for RNA-seq data with DESeq2. Genome Biol. *15*, 550. https://doi.org/10.1186/s13059-014-0550-8.
46. Wei, G., Twomey, D., Lamb, J., Schlis, K., Agarwal, J., Stam, R.W., Opferman, J.T., Sallan, S.E., den Boer, M.L., Pieters, R., et al. (2006). Gene expression-based chemical genomics identifies rapamycin as a modulator of MCL1 and glucocorticoid resistance. Cancer Cell *10*, 331–342. https://doi.org/10.1016/j.ccr.2006.09.006.
47. Homminga, I., Pieters, R., Langerak, A.W., de Rooi, J.J., Stubbs, A., Verstegen, M., Vuerhard, M., Buijs-Gladdines, J., Kooi, C., Klous, P., et al. (2011). Integrated transcript and genome analyses reveal NKX2-1 and MEF2C as potential oncogenes in T cell acute lymphoblastic leukemia. Cancer Cell *19*, 484–497. https://doi.org/10.1016/j.ccr.2011.02.008.
48. Zhu, H., Dong, B., Zhang, Y., Wang, M., Rao, J., Cui, B., Liu, Y., Jiang, Q., Wang, W., Yang, L., et al. (2022). Integrated genomic analyses identify high-risk factors and actionable targets in T-cell acute lymphoblastic leukemia. Blood Sci. *4*, 16–28. https://doi.org/10.1097/bs9.0000000000000102.
49. Gopi, L.K., and Kidder, B.L. (2021). Integrative pan cancer analysis reveals epigenomic variation in cancer type and cell specific chromatin domains. Nat. Commun. *12*, 1419. https://doi.org/10.1038/s41467-021-21707-1.
50. Shi, J., Zhang, Z., Cen, H., Wu, H., Zhang, S., Liu, J., Leng, Y., Ren, A., Liu, X., Zhang, Z., et al. (2021). CAR T cells targeting CD99 as an approach to eradicate T-cell acute lymphoblastic leukemia without normal blood cells toxicity. J. Hematol. Oncol. *14*, 162. https://doi.org/10.1186/s13045-021-01178-z.
51. Yang, L., Chen, F., Zhu, H., Chen, Y., Dong, B., Shi, M., Wang, W., Jiang, Q., Zhang, L., Huang, X., et al. (2021). 3D genome alterations associated with dysregulated HOXA13 expression in high-risk T-lineage acute lymphoblastic leukemia. Nat. Commun. *12*, 3708. https://doi.org/10.1038/s41467-021-24044-5.
52. Luchtel, R.A., Bhagat, T., Pradhan, K., Jacobs, W.R., Jr., Levine, M., Verma, A., and Shenoy, N. (2020). High-dose ascorbic acid synergizes with anti-PD1 in a lymphoma mouse model. Proc. Natl. Acad. Sci. USA *117*, 1666–1677. https://doi.org/10.1073/pnas.1908158117.

STAR★METHODS

KEY RESOURCES TABLE

REAGENT or RESOURCE	SOURCE	IDENTIFIER
Antibodies		
β-Tubulin Rabbit mAb	ABclonal	Cat#A12289; RRID: AB_2861647
HRP Goat Anti-Mouse IgG (H+L)	ABclonal	Cat#AS003; RRID: AB_2769851
HRP Goat Anti-Rabbit IgG (H+L)	ABclonal	Cat#AS014; RRID: AB_2769854
c-Jun Rabbit pAb	ABclonal	Cat#A11378; RRID: AB_2758533
c-Jun Rabbit pAb	ABclonal	Cat#A0246; RRID: AB_2757059
JNK1/2/3 Rabbit pAb	ABclonal	Cat#A18678; RRID: AB_2862414
Phospho-JNK1/2-T183/Y185 Rabbit pAb	ABclonal	Cat#AP0473; RRID: AB_2771231
p38 MAPK Rabbit pAb	ABclonal	Cat#A10832; RRID: AB_2758256
Phospho-p38 MAPK-T180 Rabbit pAb	ABclonal	Cat#AP1434
GAPDH Monoclonal antibody	Proteintech	Cat#60004-1-Ig; RRID: AB_2107436
HA tag Polyclonal antibody	Proteintech	Cat#51064-2-AP; RRID: AB_11042321
HIF-1 alpha Polyclonal antibody	Proteintech	Cat# 20960-1-AP; RRID: AB_10732601
HRP-conjugated IgG Fraction Monoclonal Mouse Anti-Rabbit IgG, Light Chain Specific	Proteintech	Cat# SA00001-7L; RRID: AB_2890988
DYKDDDDK tag Monoclonal antibody	Proteintech	Cat# 66008-4-Ig; RRID: AB_2918475
BV421 Mouse Anti-Human CD7	BD Biosciences	Cat#562635; RRID: AB_2736907
p44/42 MAPK (Erk1/2) Antibody	Cell Signaling Technology	Cat#9102
Phospho-p44/42 MAPK (Erk1/2) (Thr202/Tyr204) (D13.14.4E) XP® Rabbit mAb	Cell Signaling Technology	Cat#8544
Bcl-xL (54H6) Rabbit mAb	Cell Signaling Technology	Cat#2764
Bax (E4U1V) Rabbit mAb	Cell Signaling Technology	Cat#41162
Bacterial and virus strains		
pLKO.1-HIF1α lentivirus	This paper	N/A
pLKO.1-JUN lentivirus	This paper	N/A
pLVX-HIF1α lentivirus	This paper	N/A
pLVX-JUN lentivirus	This paper	N/A
Chemicals, peptides, and recombinant proteins		
Dexamethasone	Aladdin	Cat#D137736
2-Methoxyestradiol	Aladdin	Cat#M125960
BAY 87-2243	Selleck	Cat#1227158-85-1
RPMI 1640 medium	Gibco	Cat#C11875500BT
DMEM medium	Gibco	Cat#C11995500BT
Fetal Bovine Serum	Gibco	Cat#10099141C
Critical commercial assays		
Ultima Dual-mode RNA Library Prep Kit for Illumina kit	Yeasen	Cat#12252
Hyperactive In-Situ ChIP Library Prep Kit for Illumina kit	Vazyme	Cat#TD901
ABScript III RT Master Mix for qPCR with gDNA Remover	ABclonal	Cat# RK20429
2×TSINGKE® Master qPCR Mix (SYBR Green I)	Tsingke	Cat#TSE201
Approved Drug Library	TargetMol	Cat#L1000
Cell Counting Kit-8 reagent	Yeasen	Cat#40203

(*Continued on next page*)

Continued

REAGENT or RESOURCE	SOURCE	IDENTIFIER
SteadyPure Universal RNA Extraction Kit II	Accurate Biology	Cat#AG21022
Deposited data		
Raw and analyzed data	This paper	GSA: HRA004881
Experimental models: Cell lines		
MOLT-3	ATCC	CRL-1552
MOLT-4	ATCC	CRL-1582
CCRF-CEM	ATCC	CCL-119
Loucy	ATCC	CRL-2629
Jurkat	ATCC	TIB-152
PEER	DMSZ	ACC 6
MOLT-16	DMSZ	ACC 29
KE-37	DMSZ	ACC 46
HEK-293FT	Chinese Academy of Sciences Cell Bank	SCSP-5212
CCRF-CEM(Dex)	This paper	N/A
Experimental models: Organisms/strains		
Mouse: NCG (NOD/ShiLtJGpt-Prkdc^{em26Cd52}Il2rg^{em26Cd22}/Gpt)	Gempharmatech Co., Ltd	Strain NO. T001475
Oligonucleotides		
shHIF1α-1 sequence forward: CCGGTGCTGATTTGTGAACCCA TTCCCTCGAGGGAATGGGTTCACAAATCAGCTTTTTG	This paper	N/A
shHIF1α-1 sequence reverse: AATTCAAAAAGCTGATTTGTGAA CCCATTCCCTCGAGGGAATGGGTTCACAAATCAGCA	This paper	N/A
shHIF1α-2 sequence forward: CCGGTGCCGAGGAAGAACTATG AACACTCGAGTGTTCATAGTTCTTCCTCGGCTTTTTG	This paper	N/A
shHIF1α-2 sequence reverse: AATTCAAAAAGCCGAGGAAGAAC TATGAACACTCGAGTGTTCATAGTTCTTCCTCGGCA	This paper	N/A
shJUN-1 sequence forward: CCGGTCCCATCAACATGGAAGACC AACTCGAGTTGGTCTTCCATGTTGATGGGTTTTTG	This paper	N/A
shJUN-1 sequence reverse: AATTCAAAAACCCATCAACATGGAA GACCAACTCGAGTTGGTCTTCCATGTTGATGGGA	This paper	N/A
shJUN-2 sequence forward: CCGGTGGAACAGGTGGCACAGCTT AACTCGAGTTAAGCTGTGCCACCTGTTCCTTTTTG	This paper	N/A
shJUN-2 sequence reverse: AATTCAAAAAGGAACAGGTGGCAC AGCTTAACTCGAGTTAAGCTGTGCCACCTGTTCCA	This paper	N/A
Recombinant DNA		
pcDNA3.1	Thermo Fisher Scientific	Cat#V79520
pcDNA3.1 harboring FLAG-tag sequence	This paper	N/A
pcDNA3.1 harboring HA-tag sequence	This paper	N/A
Software and algorithms		
FlowJo(software for flow cytometry analysis)	BD Biosciences	N/A
ImageJ (software for image analysis)	National Institutes of Health	N/A
GraphPad Prism 8 (software for drawing graphs and statistics analysis)	Graphpad	N/A
Trim Galore	N/A	https://www.bioinformatics.babraham.ac.uk/projects/trim_galore/

(*Continued on next page*)

Continued

REAGENT or RESOURCE	SOURCE	IDENTIFIER
deepTools	Ramírez et al.[39]	https://deeptools.readthedocs.io/en/develop/;RRID:SCR_016366
MACS2	John, M.G.[40]	https://pypi.org/project/MACS2/
IGV (software for visually analyze ChIP-seq and ATAC-seq)	James, T.[41]	https://www.nature.com/articles/nbt.1754
Bowtie2 (software for data analyze)	Langmead, B. et al.[42]	https://www.nature.com/articles/nmeth.1923#citeas
Samtools (software for data analyze)	Li et al.[43]	https://github.com/samtools/
FeatureCounts (software for data analyze)	Liao Y et al.[44]	https://subread.sourceforge.net/featureCounts.html
DESeq2	Love et al.[45]	https://bioconductor.org/packages/release/bioc/html/DESeq2.html
Others		
BD FACSAria	BD Biosciences	N/A
Raw and analyzed data	Wei G. et al.[46]	GEO: GSE5820
Raw and analyzed data	Homminga I. et al.[47]	GEO: GSE26713
Raw and analyzed data	Zhu H. et al.[48]	GSA: HRA000122
Raw and analyzed data	Gopi L.K. et al.[49]	GEO: GSE143653

RESOURCE AVAILABILITY

Lead contact

Further information and requests for resources and reagents should be directed to the lead contact, Zhu Haichuan (zhuhaichuan@wust.edu.cn).

Materials availability

The study did not generate new unique reagents.

Data and code availability

- Data：The RNA-seq and ATAC-seq data in this study have been deposited in the Genome Sequence Archive (GSA) for human under accession number HRA004881, which is publicly available. The transcriptomic and clinical data of T-ALL patients cohort was retrieved from Genome Sequence Archive (GSA) for human under accession number HRA000122 which our previous published. GEO accession codes of the published data used in this study are as follows: The data of Glucocorticoid resistance in T-ALL patients, GEO: GSE5820; The data of T-ALL samples compared to normal BM samples, GEO: GSE26713; H3K27ac and H3K4me3 ChIP-seq of CCRF-CEM cell line, GEO: GSE143653.
- Code：This paper does not report original code.
- Any additional information required to reanalyze the data reported in this paper is available from the lead contact upon request.

EXPERIMENTAL MODEL AND STUDY PARTICIPANT DETAILS

Cell lines and growth condition

Jurkat, MOLT-3, MOLT-4, CCRF-CEM, Loucy, PEER, MOLT-16, CUTLL-1 and KE-37 cells were cultured in RPMI-1640 (Gibco, C11875500BT) with 10% FBS (Gibco, 10099-141), and HEK-293T cells were cultured in DMEM (Gibco, C11995500BT) with 10% FBS (Gibco, 10099141C). All these cells were confirmed by STR profiling analysis, tested negative for mycoplasma, and cultured in at 37°C with 5% CO_2.

Patients samples

The T-ALL samples were collected from diagnostic bone marrow at the Zhongnan Hospital of Wuhan University of China. The patient characteristics are described in Table S1. This study was approved by the Ethics Committee of Zhongnan Hospital of Wuhan University (No.2020201). All patients provided written informed consent before any study procedure.

Mouse models

The 6- to 8-week-old male NCG mice (Strain NO. T001475, NOD/ShiLtJGpt-Prkdc^{em26Cd52}Il2rg^{em26Cd22}/Gpt) were purchased from GemPharmatech (Nanjing, China). This *in vivo study* was approved by the Animal Ethics Committee of Wuhan University of Science and Technology(No.WKD-Zhu-03). The protocol for CCRF-CEM(Dex) cell-derived CDX models and T5 T-ALL patient cell-derived PDX models has been described previously.[50] First, CDX mice were treated with dexamethasone 30 mg/kg/2 days (Aladdin, 50-02-2), 2-MeOE2 30 mg/kg/2 days (Aladdin, 362-07-2) or a combination of dexamethasone and 2-methoxyestradiol intraperitoneally. PBS buffer was used as a control. The endpoint of the experiments was that weight loss exceeded 20% of the body weight of a similar normal animal according to the guidelines of the Canadian Council on Animal Care (CCAC).

METHOD DETAILS

Gene knockdown and overexpression

Gene knockdown was performed through short hairpin RNA (shRNA) based on lentiviral vectors as described previously.[50] Gene knockdown was performed through short hairpin RNA (shRNA), the shRNA sequences of HIF1α and JUN were cloned into a pLKO.1 lentiviral vector. Then, Jurkat and CCRF-CEM(Dex) cells were infected with lentivirus packaged by the silencing plasmid (pLKO.1-puro), which includes a puromycin resistance region, and an shRNA construct to target HIF1α and JUN or a non-specific shRNA control (shRNA C: 5′-CAACACAGATGATAGAG CACCAATTGGTGCTCTATCATCTGTGTTGTTTTT-3′). The primer sequences of shRNA are discussed in key resources table. For HIF1α and JUN overexpression, the CDS sequence was cloned into a pLVX lentiviral vector. Lentiviruses were generated by cotransfecting target plasmids with the helper plasmids into HEK-293FT cells using polyethylenimine.

Real time PCR

RNA was extracted using SteadyPure Universal RNA Extraction Kit II (AG, AG21022) and cDNA was synthesized using ABScript III RT Master Mix for qPCR with gDNA Remover (ABclonal, RK20429). RT-PCR was performed in triplicate using 2×TSINGKE® Master qPCR Mix (SYBR Green I) (TSINGKE, TSE201).

Coimmunoprecipitation and western blot analysis

Coimmunoprecipitation cells were lysed in lysis buffer (50 mM HEPES, pH 7.5, 10% glycerol, 150 mM NaCl, 1% Triton X-100, 1 mM EDTA, 1 mM EGTA, 10 mM NaF and 30 mM b-glycerolphosphate), followed by immunoprecipitation using beads conjugated to the desired antibody. After overnight incubation at 4°C with beads, the samples were washed three times, and proteins were eluted using 5× protein sample buffer followed by immunoblotting. Standard procedures were used for Western blotting analysis. Cells were lysed in RIPA lysis buffer and stabilized in 5× protein sample buffer. Proteins were resolved using SDS-polyacrylamide gel electrophoresis, transferred to PVDF membranes, and probed with the antibodies listed in method. The secondary antibodies used were anti-rabbit and anti-mouse IgG horseradish peroxidase-linked whole antibodies from ABclonal.

Flow cytometry

Flow cytometry was performed using a Beckman CytoFLEX flow cytometer. FACS sorting was performed using a BD FACSAria (BD Biosciences, USA). Peripheral blood mononuclear cells (PBMCs) were lysed with red blood cell (RBC) lysis buffer to remove the red blood cells to obtain mononuclear cell suspensions and prepared through the process described above. Peripheral blood and bone marrow cells were collected, washed and then incubated with anti-human CD7 antibody (BD Biosciences, 562635) for 30 min at 4°C. Cells were subsequently stained with 7-AAD to exclude dead cells. Positive events were determined by isotype control gating for each antibody. Data analysis was carried out using FlowJo (v10.0.7, FlowJo, LLC, Ashland, OR, USA).

RNA-seq analysis

The RNA-seq analysis has been described previously.[51] CCRF-CEM and CCRF-CEM(Dex) were prepared three samples of each cell line for RNA library construction. Then, RNA libraries of 300–400 bp were generated with the Ultima Dual-mode RNA Library Prep Kit for Illumina kit (Yeasen, 12252ES24). These libraries were subjected to 150 bp paired-end sequencing using a NovaSeq 6000 platform.

Reads were aligned to the hg38 genome with STAR, and protein-coding genes were calculated using DESeq2 to generate TPM from reads of each gene. Differentially expressed genes (DEGs) were selected with $p < 0.05$ and $|\log2 \text{Fold Change}| > 0.5$. KEGG signalling enrichment was performed by clusterProfiler. Transcription factor (TF) enrichment analysis was performed by ChEA3 with the ReMap Chip-seq library. Activity analysis of transcription factors (TFs) was performed by DoRothEA.

ATAC-seq analysis

ATAC-seq analysis has been described previously[43,51] ATAC-seq libraries with Hyperactive In-Situ ChIP Library Prep Kit for Illumina (Vazyme, TD 901) according to its protocol, then the ATAC-seq libraries were sequenced.

Clean data were generated by Trim Galore. ATAC-seq reads were aligned to the hg38 genome with Bowtie2. Then, BAM files were generated, PCR duplicates were removed by Sambamba, and mitochondrial genomes were filtered out by Samtools. Signal peaks were generated by MACS2. Motif analysis was performed by using findMotifs.pl of HOMER.

Drug library screening

To screen the drugs that were sensitive to dexamethasone-resistant cells, we first screened the Approved Drug Library (TargetMol, L1000) using Jurkat and CCRF-CEM cells. In brief, 2×10^4 cells were seeded in flat tissue culture plates (96 wells) and treated with each drug of the library (3 μM) for 48 hours. An equal volume of DMSO was added synchronously as the negative control. To examine cell viability, the cells were incubated with Cell Counting Kit-8 reagent (Yeasen, 40203ES92) following the manufacturer's protocol and then detected at 450 nm (OD). Then, 2×10^4 CCRF-CEM or CCRF-CEM(Dex) cells were seeded in flat tissue culture plates (96 wells) and treated with each drug of the library (1 μM) for 48 hours, incubated with CCK-8 and detected at 450 nm (OD). Selected drugs with stronger inhibitory effects on CCRF-CEM(DEX) cells were selected for secondary screening. The synergy of dexamethasone and HIF1α inhibitors was measured by the coefficient of drug interaction (CDI), and a CDI <1 indicated a synergistic effect.[52]

QUANTIFICATION AND STATISTICAL ANALYSIS

Specific statistical analyses have been described in each section. For cell experiments, statistical significance between two groups was determined by unpaired Student's *t* test. One-way ANOVA was used to examine more than two groups. Three independent replicates were performed unless otherwise specified, and data are represented as means ± SD. Statistical analyses were calculated using GraphPad Prism. For clinical survival data analysis, the optimal cut-off values were determined using the maximally selected rank statistics, and the survival curves were tested with the log rank test.